Int. J. Heat Mass Transfer. Vol. 36, No. 5, pp. 1241–1250, 1993
Printed in Great Britain

0017-9310/93 $6.00+0.00

Natural convection near a corner of an arbitrary angle formed by two vertical flat plates with uniform surface heat flux

MAN HOE KIM,† MOON-UHN KIM‡ and CHUL HYUNG CHO†

† Division of Mechanical Engineering and ‡ Department of Applied Mathematics, Korea Advanced Institute of Science and Technology, P.O. Box 150, Cheongryang, Seoul, Korea

(*Received* 21 *January* 1991 *and in final form* 13 *January* 1992)

Abstract—The laminar natural convection flow along a corner of an arbitrary angle formed by two vertical flat plates with uniform surface heat flux is considered. For large modified Grashof numbers, the leading order corner layer equations and appropriate boundary conditions are formulated in an oblique coordinate system using the method of matched asymptotic expansions. The analysis is valid mathematically for any corner angle, $0° < \alpha_c < 360°$. The velocity and temperature distributions for Prandtl numbers 0.733 (air) and 6.7 (water) are obtained using the ADI-type finite difference technique for corner angles ranging from 90° to 270°. The general features of the solutions are similar to those with isothermal wall conditions except for the temperature profiles in the vicinity of the corner.

1. INTRODUCTION

As a fundamental problem of three-dimensional boundary layer flows, the high Reynolds number flow along a corner formed by two quarter-infinite flat plates with co-planar leading edges has been analyzed by several authors [1–6] since the work by Carrier [1]. On the other hand, the heat transfer characteristics of three-dimensional corner flows have been studied only recently: the natural convection near a concave vertical corner submerged in a saturated porous medium [7], the forced convective heat transfer in the flow along a corner of an arbitrary angle [8], the natural convection near a vertical rectangular corner with uniform surface temperature [9] or uniform surface heat flux [10], and the natural convection near an isothermal vertical corner of an arbitrary angle [11].

In the present paper, as a generalization of the earlier work [10], the laminar free convection near a vertical corner of an arbitrary angle with uniform surface heat flux is considered. For large modified Grashof numbers, the corner layer equations and the appropriate boundary conditions are derived by a method (based on the method of matched asymptotic expansions) similar to that used in refs. [6, 11]. For the numerical solution, an alternative direction implicit (ADI) scheme is employed, and results for corners of angles ranging from 90° to 270° are presented for Prandtl numbers of 0.733 (air) and 6.7 (water).

2. CORNER LAYER EQUATIONS

We consider the laminar natural convection boundary layer flow near a corner formed by the intersection of two vertical quarter-infinite planes with uniform surface heat flux. The problem is formulated in an oblique coordinate system (x_0, y_0, z_0), where the x_0-axis is vertically upward and the origin at the leading edge. Both y_0- and z_0-axes are perpendicular to the x_0-axis and lie, respectively, in the symmetry plane and in one of the joining quarter-infinite plates (Fig. 1). The coordinates are simply related to the Cartesian coordinate system (x, y, z) by

$$(x_0, y_0, z_0) = (x, y - z\tan\alpha, z/\cos\alpha). \tag{1}$$

Considering the following symmetry properties along the corner bisector (y_0-axis), it is sufficient to analyze the flow in the half region $z_0 \geqslant 0$

$$\begin{aligned} u^*(x,y,z) &= u^*(x,y,-z) \\ v^*(x,y,z) &= v^*(x,y,-z) \\ w^*(x,y,z) &= -w^*(x,y,-z) \\ T(x,y,z) &= T(x,y,-z). \end{aligned} \tag{2}$$

Employing the Boussinesq approximation and neglecting the viscous dissipation, the governing equations in the oblique coordinate system are

$$\frac{\partial u_0^*}{\partial x_0} + \frac{\partial v_0^*}{\partial y_0} + \frac{\partial w_0^*}{\partial z_0} = 0 \tag{3a}$$

$$\frac{\mathrm{D}u_0^*}{\mathrm{D}t} = -\frac{1}{\rho}\frac{\partial p_0^*}{\partial x_0} + \nu\nabla^{*2}u_0^* + g\beta(T - T_\infty) \tag{3b}$$

$$\frac{\mathrm{D}}{\mathrm{D}t}(v_0^* + w_0^*\sin\alpha) = -\frac{1}{\rho}\frac{\partial p_0^*}{\partial y_0} + \nu\nabla^{*2}(v_0^* + w_0^*\sin\alpha) \tag{3c}$$

$$\frac{\mathrm{D}}{\mathrm{D}t}(w_0^* + v_0^*\sin\alpha) = -\frac{1}{\rho}\frac{\partial p_0^*}{\partial z_0} + \nu\nabla^{*2}(w_0^* + v_0^*\sin\alpha) \tag{3d}$$

$$\frac{\mathrm{D}T}{\mathrm{D}t} = \kappa\nabla^{*2}T \tag{3e}$$

NOMENCLATURE

a = 0.2, grid spacing parameter
Gr^* local modified Grashof number, $g\beta q_w x_0^4/kv^2$
k thermal conductivity of fluid
N, S transformed independent variables
Nu local Nusselt number
p_0^* pressure in x_0, y_0, z_0 coordinate system
p pressure in ξ, η, ζ coordinate system
Pr Prandtl number, v/κ
q_w surface heat flux
r magnitude of crossflow velocity, $(Gr^*/5)^{1/5}(v^{*2}+w^{*2})^{1/2}/U_c$
T temperature
T_∞ ambient temperature
ΔT temperature difference, $T_w - T_\infty$
u_0^*, v_0^*, w_0^* velocity components in x_0, y_0, z_0 directions
u^*, v^*, w^* velocity components in x, y, z directions
u, v, w velocity components in ξ, η, ζ directions
U_c convective velocity, $(v/x_0)(Gr^*/5)^{2/5}$
x_0, y_0, z_0 oblique coordinate system defined in Fig. 1
x, y, z Cartesian coordinate system.

Greek symbols
α = $\frac{1}{2}(\pi - \alpha_c)$
α_c corner angle
β thermal expansion coefficient
γ = $\lim_{\eta\to\infty}[-4f(\eta)]$
θ dimensionless temperature
κ thermal diffusivity
μ dynamic viscosity
ν kinematic viscosity, μ/ρ
ξ, η, ζ scaled independent variables
ρ density of fluid
τ_w wall shear stress
$\tau_{w\infty}$ wall shear stress as $\zeta \to \infty$
ϕ, ψ velocity potentials defined in equation (6)
Ω modified vorticity function defined in equation (6).

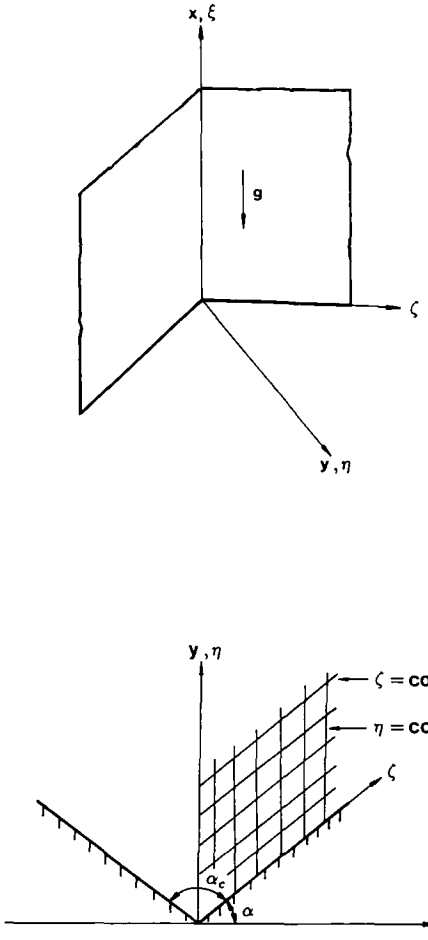

FIG. 1. Definition sketch.

where

$$\frac{D}{Dt} \equiv u_0^* \frac{\partial}{\partial x_0} + v_0^* \frac{\partial}{\partial y_0} + w_0^* \frac{\partial}{\partial z_0}$$

$$\nabla^{*2} \equiv \frac{\partial^2}{\partial x_0^2} + \frac{1}{\cos^2\alpha}\left(\frac{\partial^2}{\partial y_0^2} - 2\sin\alpha \frac{\partial^2}{\partial y_0 \partial z_0} + \frac{\partial^2}{\partial z_0^2}\right).$$

In order to obtain the leading order corner layer equations, we introduce the following corner layer variables [10]:

$$[u(\eta,\zeta), v(\eta,\zeta), w(\eta,\zeta)] = \left[\frac{u_0^*}{U_c}, \frac{v_0^*}{U_c}\left(\frac{Gr^*}{5}\right)^{1/5}, \frac{w_0^*}{U_c}\left(\frac{Gr^*}{5}\right)^{1/5}\right]$$

$$p(\eta,\zeta) = \frac{p_0^*}{\rho U_c^2}\left(\frac{Gr^*}{5}\right)^{2/5}$$

$$\theta(\eta,\zeta) = \frac{k}{q_w x_0}(T - T_\infty)\left(\frac{Gr^*}{5}\right)^{1/5}$$

$$\eta = \frac{y_0}{x_0}\left(\frac{Gr^*}{5}\right)^{1/5}, \quad \zeta = \frac{z_0}{x_0}\left(\frac{Gr^*}{5}\right)^{1/5} \tag{4}$$

where Gr^* and U_c denote, respectively, the modified Grashof number and the convective velocity

$$Gr^* = g\beta q_w x_0^4/kv^2$$

$$U_c = (v/x_0)\left(\frac{Gr^*}{5}\right)^{2/5}.$$

Under the assumption that the modified Grashof

number Gr^* is sufficiently large, we obtain the following corner layer equations, by substituting equations (4) into equations (3) and retaining the leading order terms in each equation

$$-\frac{1}{5}(\eta u_\eta+\zeta u_\zeta-3u)+v_\eta+w_\zeta=0 \tag{5a}$$

$$-\frac{u}{5}(\eta u_\eta+\zeta u_\zeta-3u)+vu_\eta+wu_\zeta=\bar{\nabla}^2u+5\theta \tag{5b}$$

$$-\frac{u}{5}(\eta\bar{v}_\eta+\zeta\bar{v}_\zeta+\bar{v})+v\bar{v}_\eta+w\bar{v}_\zeta=-p_\eta+\bar{\nabla}^2\bar{v} \tag{5c}$$

$$-\frac{u}{5}(\eta\bar{w}_\eta+\zeta\bar{w}_\zeta+\bar{w})+v\bar{w}_\eta+w\bar{w}_\zeta=-p_\zeta+\bar{\nabla}^2\bar{w} \tag{5d}$$

$$-\frac{u}{5}(\eta\theta_\eta+\zeta\theta_\zeta-\theta)+v\theta_\eta+w\theta_\zeta=\frac{1}{Pr}\bar{\nabla}^2\theta \tag{5e}$$

where

$$\bar{v}\equiv v+w\sin\alpha,\quad \bar{w}\equiv w+v\sin\alpha$$

$$\bar{\nabla}^2\equiv\frac{1}{\cos^2\alpha}\left(\frac{\partial^2}{\partial\eta^2}-2\sin\alpha\frac{\partial^2}{\partial\eta\partial\zeta}+\frac{\partial^2}{\partial\zeta^2}\right).$$

Eliminating the pressure term in equations (5c) and (5d) by cross differentiation and introducing 'the velocity potentials' ϕ and ψ and 'the modified vorticity' Ω,

$$\phi=\left(\frac{\eta u}{5}-v\right)\cos\alpha,\quad \psi=\left(\frac{\zeta u}{5}-w\right)\cos\alpha,$$

$$\Omega=\frac{1}{\cos^2\alpha}[(\psi_\eta-\phi_\zeta)+(\phi_\eta-\psi_\zeta)\sin\alpha] \tag{6}$$

we have following Poisson-type equations for the flow in the corner layer:

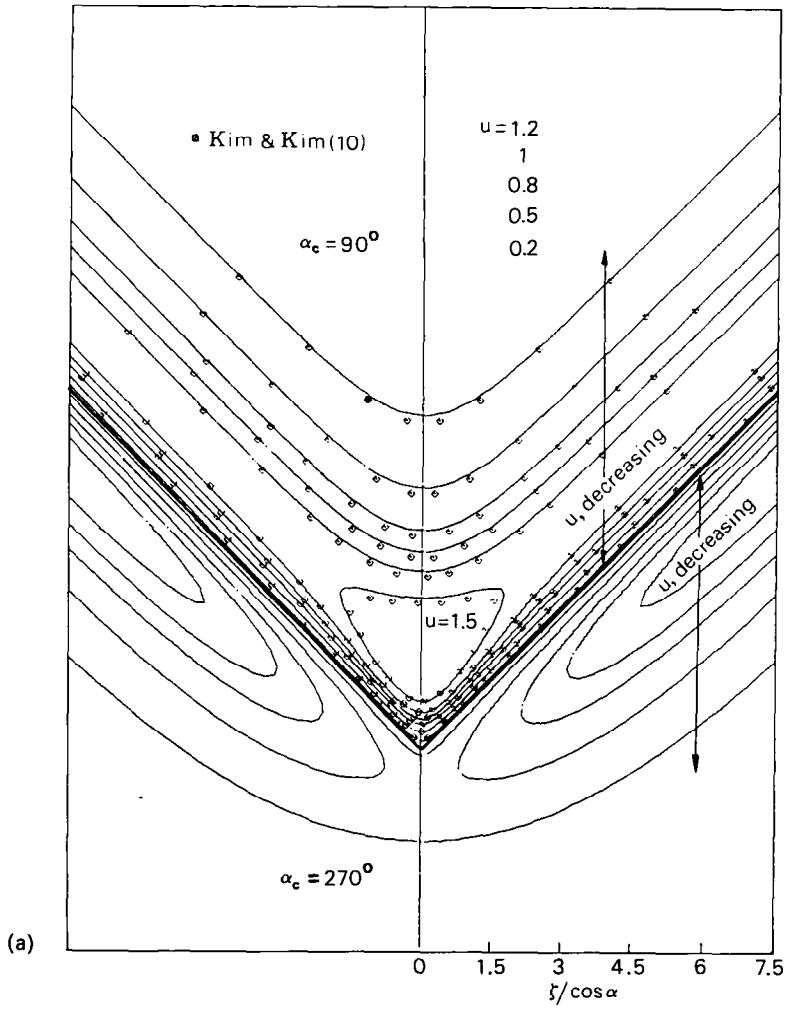

(a)

FIG. 2. Streamwise isovels for $\alpha_c = 90°$ and 270°: (a) $Pr = 0.733$; (b) $Pr = 6.7$.

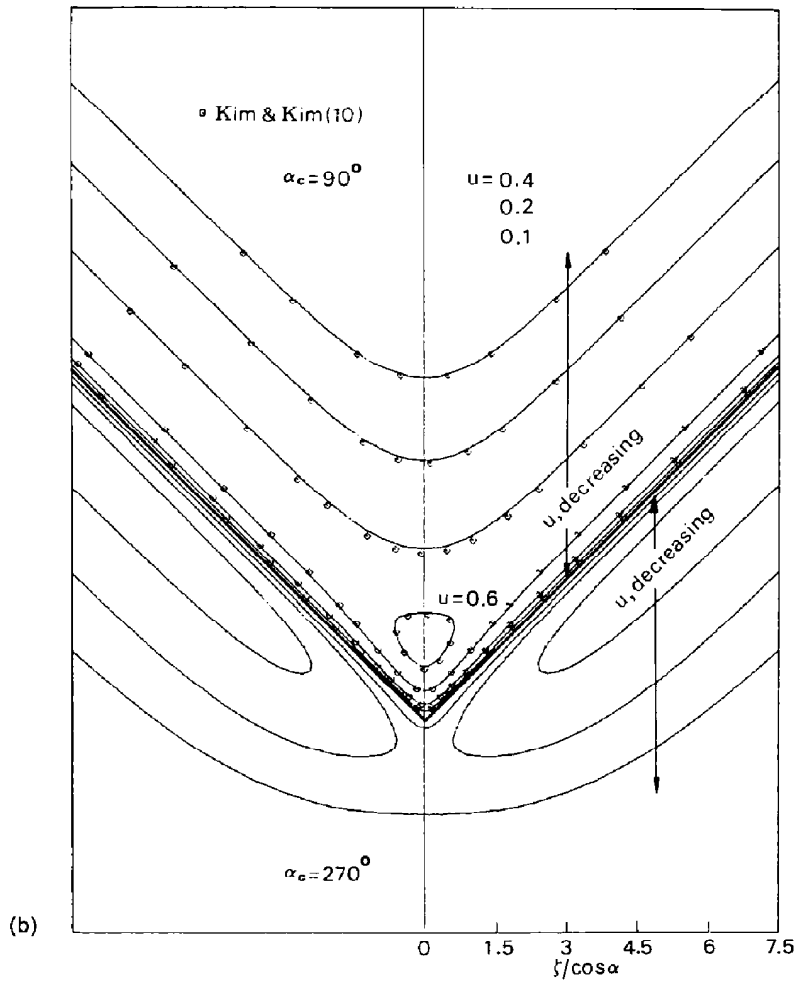

FIG. 2—*Continued.*

$$\nabla^2 u+\phi u_\eta+\psi u_\zeta-\tfrac{3}{5}\cos\alpha u^2+5\theta\cos\alpha=0$$

$$\nabla^2\Omega+\phi\Omega_\eta+\psi\Omega_\zeta+u[\Omega\cos\alpha+\tfrac{8}{25}(\eta+\zeta\sin\alpha)u_\eta-\tfrac{8}{25}(\zeta+\eta\sin\alpha)u_\zeta]+(\zeta+\eta\sin\alpha)\theta_\eta-(\eta+\zeta\sin\alpha)\theta_\zeta=0$$

$$\phi_{\eta\eta}-\phi_{\eta\zeta}\sin\alpha+\phi_{\zeta\zeta}+\psi_{\zeta\zeta}\sin\alpha+\Omega_\zeta\cos^2\alpha-u_\eta\cos\alpha=0$$

$$\psi_{\eta\eta}-\psi_{\eta\zeta}\sin\alpha+\psi_{\zeta\zeta}+\phi_{\eta\eta}\sin\alpha-\Omega_\eta\cos^2\alpha-u_\zeta\cos\alpha=0$$

$$\frac{1}{Pr}\nabla^2\theta+\phi\theta_\eta+\psi\theta_\zeta-\frac{\cos\alpha}{5}u\theta=0 \qquad (7)$$

where

$$\nabla^2\equiv\frac{1}{\cos\alpha}\left(\frac{\partial^2}{\partial\eta^2}-2\sin\alpha\frac{\partial^2}{\partial\eta\partial\zeta}+\frac{\partial^2}{\partial\zeta^2}\right).$$

It is observed that the corner layer equations (7) are similar to those for the isothermal case [11].

3. BOUNDARY CONDITIONS

Since the corner layer equations are elliptic, the boundary conditions must be specified on the entire boundaries, i.e. $\eta=0$, $\zeta=0$, $\eta\to\infty$ and $\zeta\to\infty$.

3.1. *Conditions on the wall*, $\eta=0$

On the wall, no-slip and uniform heat flux conditions are to be satisfied

$$u=\phi=\psi=0,\quad \Omega=\frac{1}{\cos^2\alpha}\psi_\eta$$

$$\theta_\eta=-\cos\alpha. \qquad (8)$$

3.2. *Conditions on the symmetry plane*, $\zeta=0$

By noting symmetry properties (2), the conditions on the symmetry plane are given as

$$u_\zeta-u_\eta\sin\alpha=0,\qquad \Omega=\psi=0,$$

$$\phi_\zeta-(\phi_\eta-\psi_\zeta)\sin\alpha=0,\quad \theta_\zeta-\theta_\eta\sin\alpha=0. \qquad (9)$$

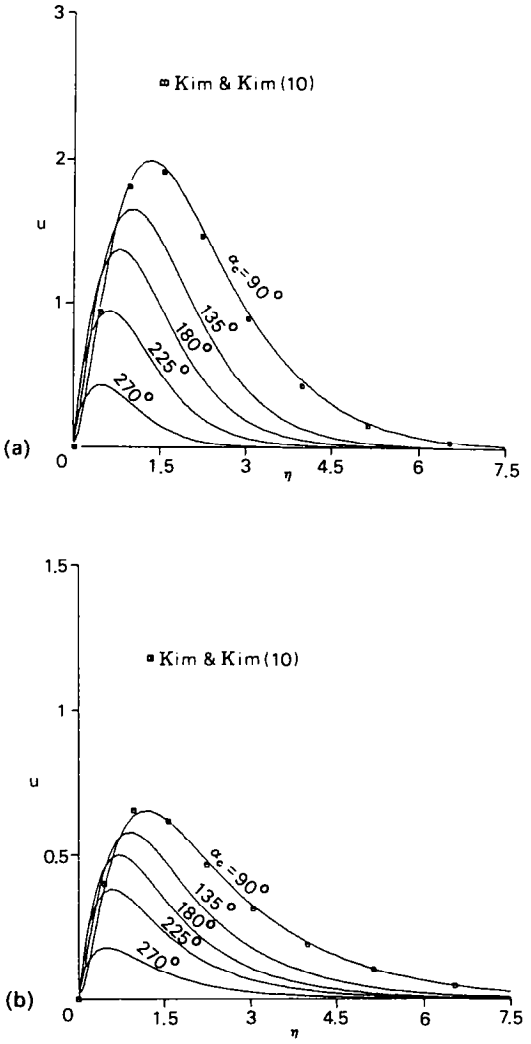

FIG. 3. Streamwise velocity profiles in the symmetry plane for various corner angles: (a) $Pr = 0.733$; (b) $Pr = 6.7$.

3.3. *Conditions as* $\eta \to \infty$

As $\eta \to \infty$, the corner layer approaches the inner edge of the outer inviscid isothermal region. In the same manner as in ref. [11], the conditions as $\eta \to \infty$ are shown to be

$$u \sim 0, \quad \Omega \sim 0, \quad \phi \sim -\gamma \cos\alpha, \quad \psi \sim 0, \quad \theta \sim 0 \tag{10}$$

where γ is a constant to be determined by the matching with the value of ϕ as $\zeta \to \infty$.

3.4. *Conditions as* $\zeta \to \infty$

The far-field boundary conditions as $\zeta \to \infty$ can be obtained by matching the corner layer to the boundary layer. Considering the results for the rectangular corner [10], the following formal asymptotic expansions are seen to be adequate for the present problem [4, 6, 11]:

$$\begin{aligned} u &\sim u_0(\eta) + u_1(\eta)/\zeta + \cdots \\ \Omega &\sim \zeta\Omega_0(\eta) + \Omega_1(\eta) + \cdots \\ \phi &\sim \phi_0(\eta) + \phi_1(\eta)/\zeta + \cdots \\ \psi &\sim \zeta\psi_0(\eta) + \psi_1(\eta) + \cdots \\ \theta &\sim \theta_0(\eta) + \theta_1(\eta)/\zeta + \cdots \end{aligned} \tag{11}$$

Substituting equations (11) into equations (7) and solving the resulting equation up to the second order, we obtain the appropriate matching conditions for the corner layer variables

$$\begin{aligned} u &\sim 5f'(\eta) \\ \Omega &\sim \zeta f''(\eta)/\cos\alpha + 3f'(\eta)\tan\alpha + \psi_1'(\eta)/\cos^2\alpha \\ \phi &\sim 4f(\eta)\cos\alpha \\ \psi &\sim \zeta f'(\eta)\cos\alpha + \psi_1(\eta) \\ \theta &\sim t(\eta). \end{aligned} \tag{12}$$

Here $f(\eta)$ and $t(\eta)$ are the well-known solutions for

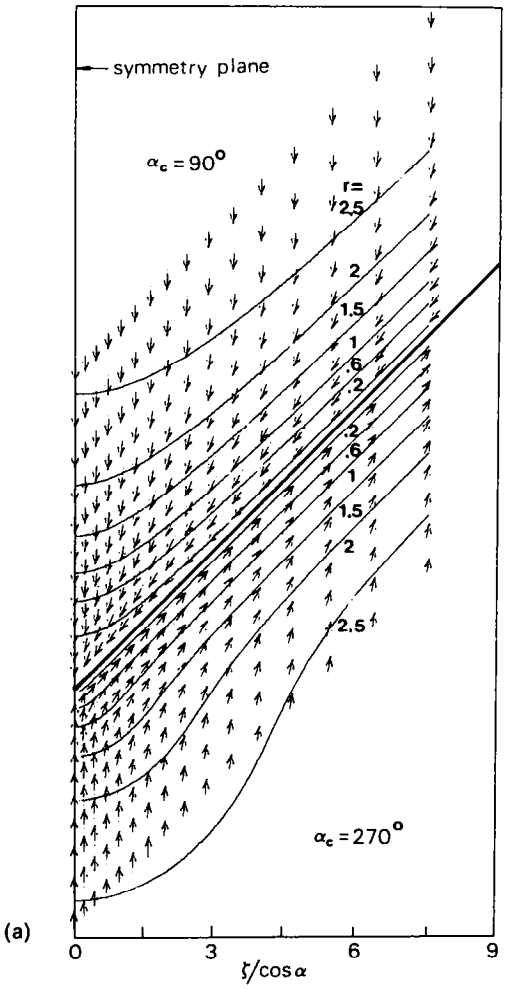

FIG. 4. Magnitudes and directions of crossflow for $\alpha_c = 90°$ and 270°: (a) $Pr = 0.733$; (b) $Pr = 6.7$.

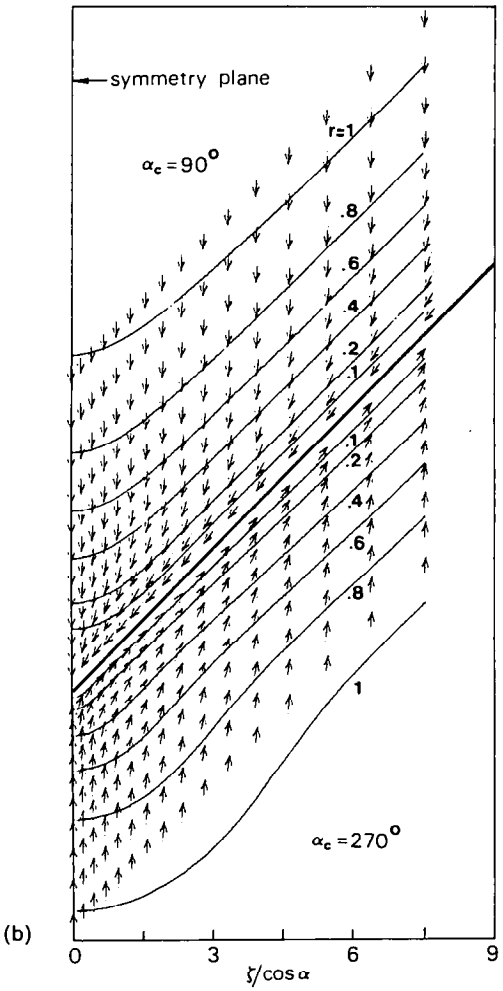

FIG. 4—*Continued.*

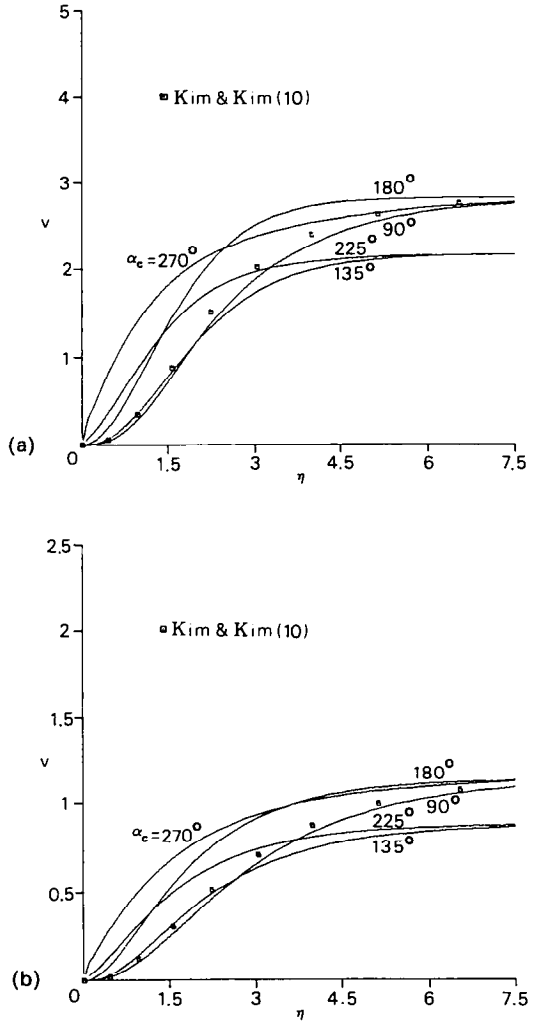

FIG. 5. Crossflow profiles in the symmetry plane for various corner angles: (a) $Pr = 0.733$; (b) $Pr = 6.7$.

the natural convection flow on a semi-infinite vertical flat plate with uniform surface heat flux, i.e.

$$f'''(\eta)+4f(\eta)f''(\eta)\cos^2\alpha-3[f'(\eta)]^2\cos^2\alpha + t(\eta)\cos^2\alpha = 0$$

$$t''(\eta)+Pr\cos^2\alpha[4f(\eta)t'(\eta)-f'(\eta)t(\eta)] = 0$$

$$f(0)=f'(0)=0, \quad t'(0) = -\cos\alpha \quad \text{and} \quad f'(\infty)=t(\infty)=0 \quad (13)$$

and the equation for $\psi_1(\eta)$ is given by

$$\psi_1''(\eta)/\cos^2\alpha+4f(\eta)\psi_1'(\eta)+f'(\eta)\psi_1(\eta) = \int_\eta^\infty h(\xi)\,d\xi$$

$$\psi_1(0)=0, \quad \psi_1(\infty)=0 \quad (14)$$

where

$$h(\xi) = [4f''(f-\xi f')+9(f')^2+\xi t'/2-t/2]\sin 2\alpha.$$

The value of γ in equation (10) can now be determined by requiring that ϕ of equation (10) be equal to that of equation (12) as $\eta \to \infty$

$$\gamma = \lim_{\eta\to\infty}[-4f(\eta)].$$

4. METHOD OF SOLUTION

The corner layer problem described in the previous section is to be solved in the infinite region $0 \leqslant \eta, \zeta \leqslant \infty$. As seen from equations (12), corner layer variables Ω and ψ become unbounded as $\zeta \to \infty$. For computational purposes, it is convenient to introduce new variables $\bar{\Omega}$ and $\bar{\psi}$ instead of Ω and ψ

$$\bar{\Omega} = \Omega-\zeta f''(\eta)/\cos\alpha, \quad \bar{\psi} = \psi-\zeta f'(\eta)\cos\alpha \quad (15)$$

and transform the infinite region $0 \leqslant \eta, \zeta \leqslant \infty$ into a finite computational domain $0 \leqslant N, S \leqslant 1$ [12]

$$N = \frac{a\eta}{1+a\eta}, \quad S = \frac{a\zeta}{1+a\zeta} \quad (16)$$

where a is a grid-spacing parameter. Transformation (16) is expected to give the improved accuracy of the numerical solution since grid points are concentrated near the corner region where large gradients are expected.

The corner layer equations and the boundary conditions are rewritten in terms of the new defined variables and are solved by the alternate direction implicit (ADI) scheme used in refs. [9–11].

5. RESULTS AND DISCUSSION

Numerical results are obtained for five corner angles ranging from 90° to 270° for two different Prandtl numbers, 0.733 and 6.7. In order to assess the accuracy of the numerical procedures, including the effect of the obliqueness of the coordinate system, the results for the rectangular corner are compared with those of Kim and Kim [10]. Both results show satisfactory agreement.

Figure 2 illustrates the streamwise isovels for $\alpha_c = 90°$ and $\alpha_c = 270°$. The general trends are much the same as those for isothermal wall conditions [11]. For a 90° corner (generally for corner angles $\alpha_c < 180°$), closed contours of streamwise isovels appear in the vicinity of the symmetry plane near the corner. The maximum value of u occurs on the symmetry plane and is greater than that of the asymptotic two-dimensional value as $\zeta \to \infty$. On the other hand, for a 270° corner (for corner angles $\alpha_c > 180°$), the maximum value of the streamwise velocity is smaller than the corresponding two-dimensional one and no closed contour appears. The thickness of the velocity boundary layer for $\alpha_c < 180°$ ($\alpha_c > 180°$) attains its maximum (minimum) at the symmetry plane and becomes thinner (thicker) as ζ increases and ultimately approaches its asymptotic two-dimensional value. In Fig. 3, the streamwise velocity profiles in the symmetry plane are shown for various corner angles. The velocity boundary layer thickness as measured in the symmetry plane and the maximum value of u increase as the corner angle is decreased. As compared

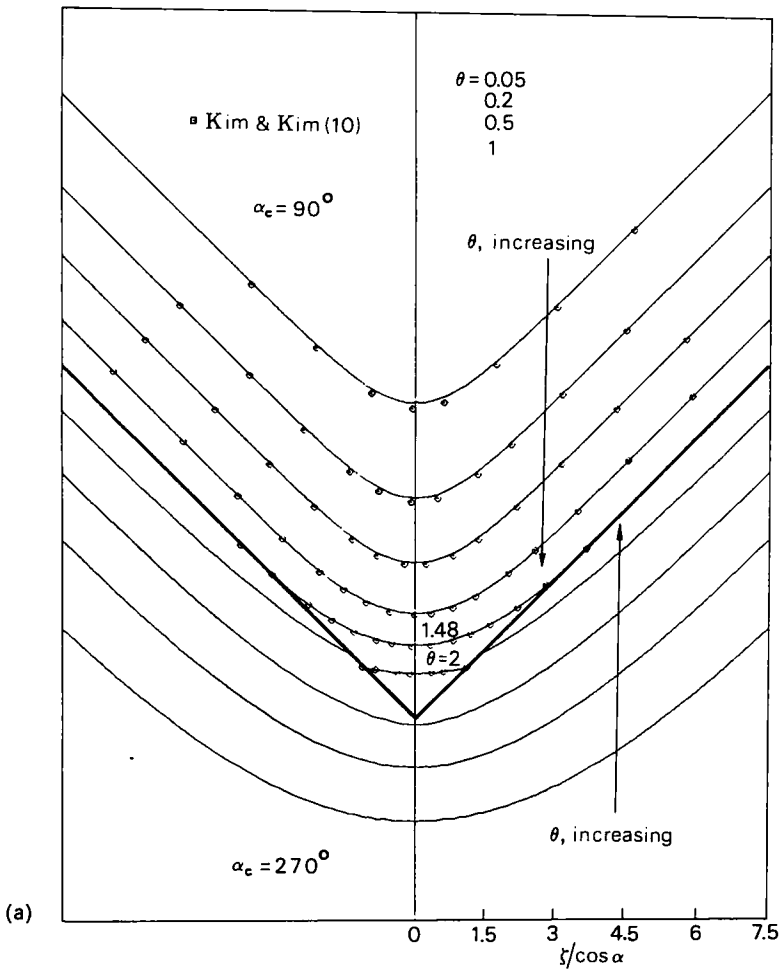

FIG. 6. Isotherms for $\alpha_c = 90°$ and 270°: (a) $Pr = 0.733$; (b) $Pr = 6.7$.

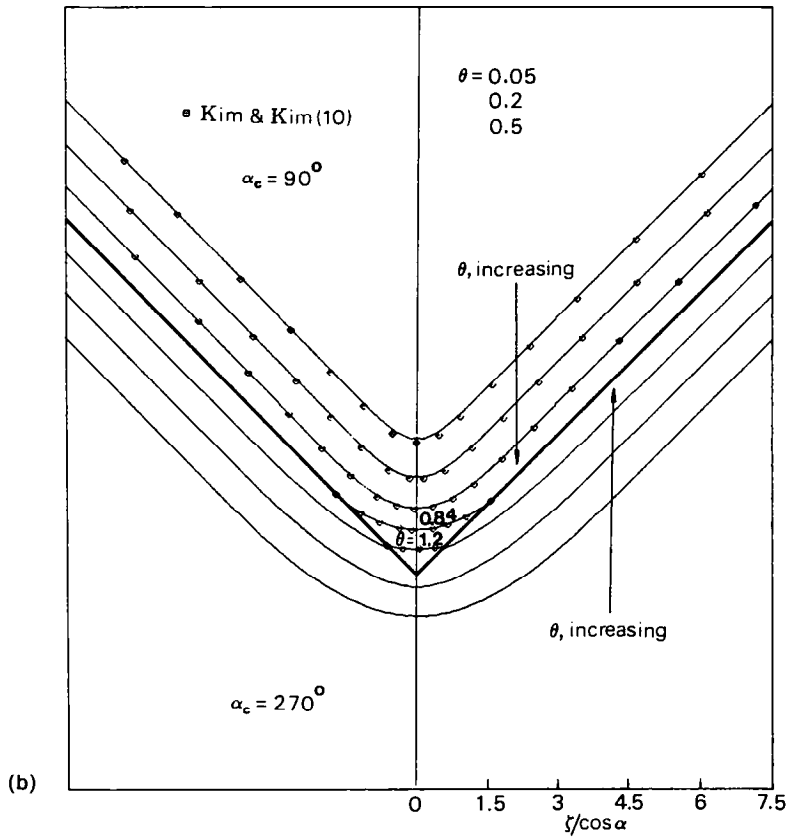

FIG. 6—*Continued.*

with the isothermal case, for isoflux walls the maximum streamwise velocity in the symmetry plane is larger for $\alpha_c < 180°$ and smaller for $\alpha_c > 180°$.

Figure 4 depicts the isolines of the scaled magnitude r and the direction of the crossflow for $\alpha_c = 90°$ and $\alpha_c = 270°$. The crossflow patterns are similar to those for isothermal walls: for $\alpha_c = 90°$ (generally for $\alpha_c < 180°$), the crossflow is converging almost radially towards the corner, while for $\alpha_c = 270°$ (generally for $\alpha_c > 180°$) the fluid in the vicinity of the symmetry plane approaches the corner and the fluid near the wall diverges outwards. Profiles of crossflow velocity v in the symmetry plane are shown in Fig. 5 for various corner angles. For $\alpha_c < 180°$, near the corner the magnitude as well as the rate of change of crossflow is larger than that for the isothermal case. Taking into consideration the equation of continuity, this behavior of crossflow distributions results in a larger variation of streamwise velocity distributions than that for uniform temperature walls.

The isothermal lines for $\alpha_c = 90°$ and 270° are depicted in Fig. 6. The surface temperature for $\alpha_c < 180°$ has a maximum value at the corner and decreases monotonically to its asymptotic two-dimensional value as the distance from the vertex increases, and vice versa for $\alpha_c > 180°$. Figure 7 shows the temperature profiles in the symmetry plane for various corner angles. It is observed that the maximum temperature in the symmetry plane is larger for smaller corner angles and decreases rapidly as α_c increases, and that the thickness of the thermal boundary layer as measured in the symmetry plane decreases as the corner angle increases. As compared with the isothermal case, the temperature gradient in the symmetry plane in larger (smaller) for the isoflux case when $\alpha_c < 180°$ ($\alpha_c > 180°$).

Figure 8 illustrates the local Nusselt number Nu defined by

$$Nu = \frac{1}{\theta(0,\zeta)}\left(\frac{Gr^*}{5}\right)^{1/5} \tag{17}$$

which shows that Nu is inversely proportional to the surface temperature $\theta(0,\zeta)$. The local Nusselt number Nu for $\alpha_c > 180°$ ($\alpha_c < 180°$) has a larger maximum (smaller minimum) value at the corner for larger (smaller) corner angles and monotonically decreases (increases) to its asymptotic two-dimensional values as ζ increases. Comparison of the curves illustrated in Fig. 8 shows that the smaller corner angle and the

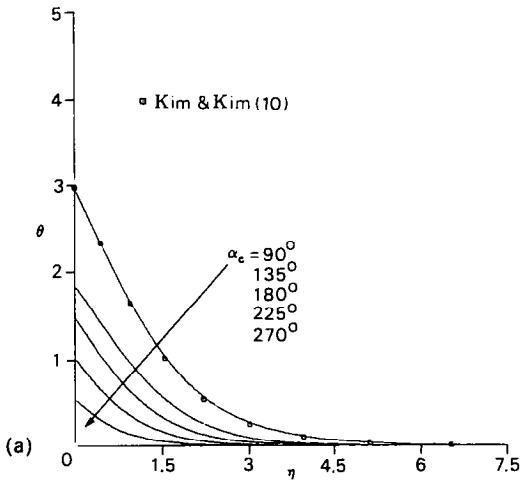

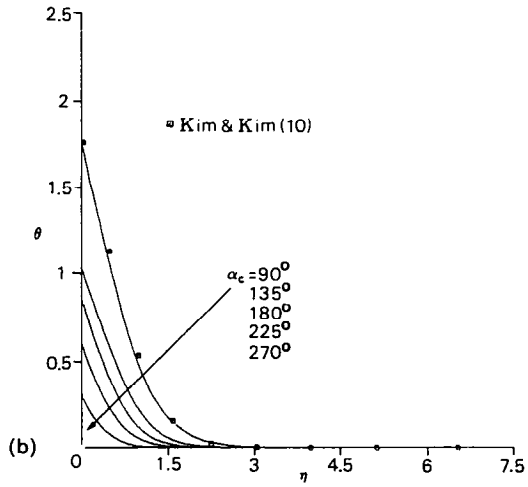

FIG. 7. Temperature profiles in the symmetry plane for various corner angles: (a) $Pr = 0.733$; (b) $Pr = 6.7$.

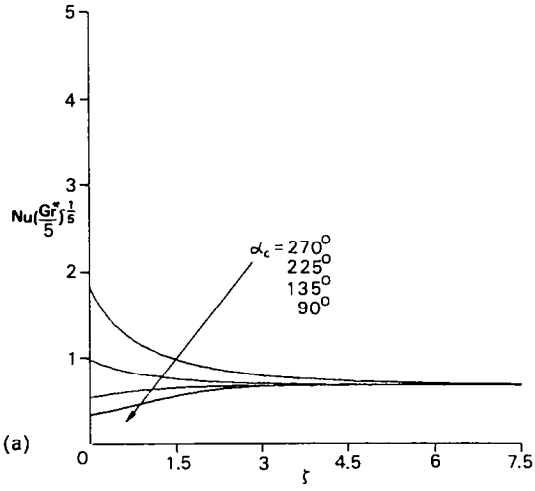

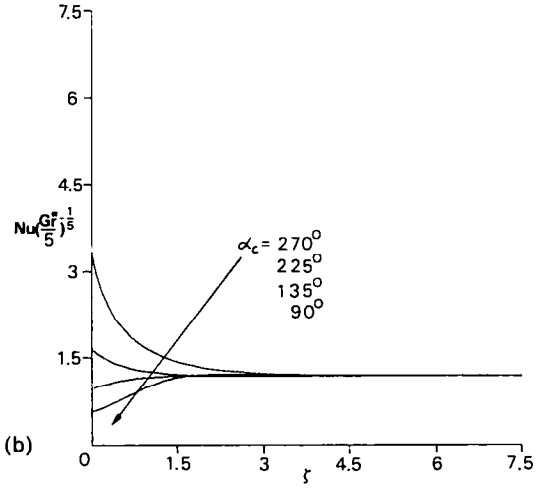

FIG. 8. Local Nusselt number distributions for various corner angles: (a) $Pr = 0.733$; (b) $Pr = 6.7$.

larger Prandtl number result in a more rapid approach to the two-dimensional value as ζ increases.

Figure 9 shows the distributions of the local shear stress given approximately by, neglecting the effect of the crossflow,

$$\tau_w = \frac{u_\eta(0,\zeta)}{\cos\alpha}\frac{\tau_{w\infty}}{f''(0)} \tag{18}$$

where $\tau_{w\infty}$ is the corresponding asymptotic two-dimensional value of τ_w

$$\tau_{w\infty} = \lim_{\zeta\to\infty}\tau_w = \frac{\rho\nu^2}{x^2}f''(0)\left(\frac{Gr^*}{5}\right)^{3/5}.$$

The qualitative behavior of τ_w with the variation of the corner angle is the same as that for isothermal wall conditions: for $\alpha_c < 180°$, τ_w is zero at the corner and attains the maximum value at a certain distance from the vertex and then decreases to its asymptotic two-dimensional value as ζ increases, and, for $\alpha_c > 180°$, τ_w decreases from a large value at the corner to its minimum and then increases to the two-dimensional value. The magnitude of overshoot (undershoot) becomes larger for greater $|\pi - \alpha_c|$.

The results given in Figs. 2–9 indicate that the qualitative features of fluid motion and heat transfer near the corner are entirely different depending on whether $\alpha_c > 180°$ or $\alpha_c < 180°$. As compared with the isothermal case, for $\alpha_c < 180°$, the streamwise velocity and the wall shear stress distributions near the corner show greater variations for the isoflux case, since near the corner the temperature varies more rapidly for the latter case and the buoyancy force becomes enhanced, the trend being more pronounced for lower Prandtl number.

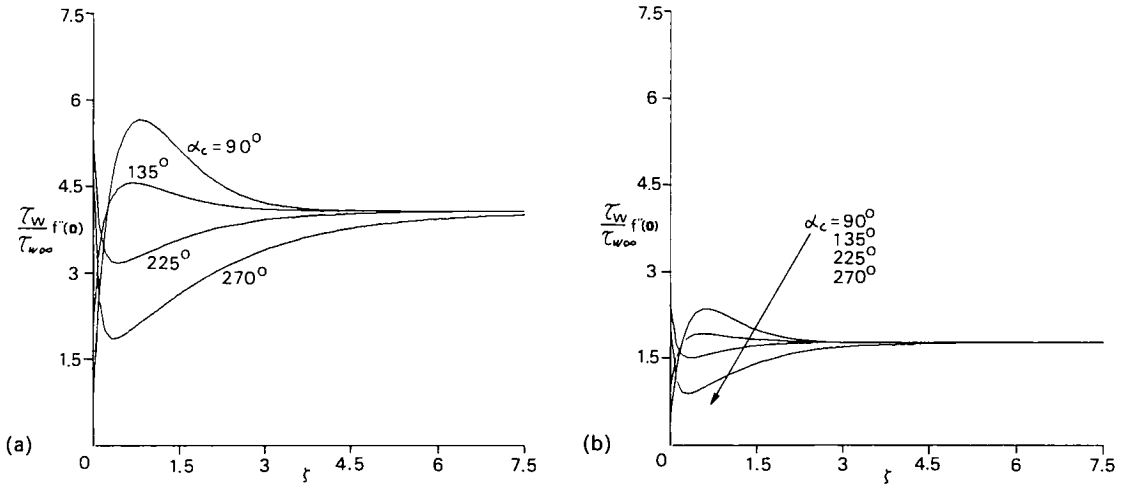

FIG. 9. Local shear stress distributions for various corner angles: (a) $Pr = 0.733$; (b) $Pr = 6.7$.

REFERENCES

1. G. F. Carrier, The boundary layer in a corner, *Quart. Appl. Math.* **12,** 367–370 (1946).
2. K. Sewartson, Viscous flow past a quarter infinite plate, *J. Aero. Sci.* **28,** 1–10 (1961).
3. S. G. Rubin, Incompressible flow along a corner, *J. Fluid Mech.* **26,** 97–110 (1966).
4. A. Pal and S. G. Rubin, Asymptotic features of viscous flow along a corner, *Quart. Appl. Math.* **29,** 91–108 (1971).
5. K. N. Ghia, Incompressible streamwise flow along an unbounded corner, *AIAA J.* **13,** 902–907 (1975).
6. W. H. Barclay and A. H. Ridha, Flow in streamwise corners of arbitrary angle, *AIAA J.* **18,** 1413–1420 (1980).
7. C. Y. Liu and A. C. Guerra, Free convection in a porous medium near the corner of arbitrary angle formed by two vertical plates, *Int. Commun. Heat Mass Transfer* **12,** 431–440 (1985).
8. M. H. Kim, M.-U. Kim and D. H. Choi, Forced convective heat transfer in the flow along a corner of arbitrary angle, *Mech. Res. Commun.* **15,** 269–274 (1988).
9. M. H. Kim and M.-U. Kim, Natural convection near a rectangular corner, *Int. J. Heat Mass Transfer* **31,** 1357–1364 (1988).
10. M. H. Kim and M.-U. Kim, Natural convection near a rectangular corner formed by two-vertical flat plates with uniform surface heat flux, *Int. J. Heat Mass Transfer* **32,** 1239–1246 (1989).
11. M. H. Kim, M.-U. Kim and D. H. Choi, Natural convection near a vertical corner of an arbitrary angle, *Int. J. Heat Mass Transfer* **34,** 1327–1336 (1991).
12. J. A. Sills, Transformations for infinite regions and their application to flow problems, *AIAA J.* **7,** 117–123 (1969).